EFFECT OF CAVITY VOLUME ON COOLING PERFORMANCE OF SYNTHETIC JET DEVICE

Hazimi Ismail, Aizat Fadzli, Ahmad Faiz Zubair, Muhammad Faris Abd Manap, Hamid Yusoff and Sh Mohd Firdaus Sh Abdul Nasir*.

Mechanical Engineering Studies, College of Engineering, Universiti Teknologi MARA, Pulau Pinang Branch, Permatang Pauh Campus, Malaysia

*Corresponding email: sh.firdaus@uitm.edu.my

Article history
Received
23rd August 2023
Revised
29th September 2023
Accepted
6th November 2023
Published
1st December 2023

ABSTRACT

Dissipating heat in a small space is a significant limitation that may cause overheating in electronic devices. A synthetic jet refers to a cooling system that does not require a fan and instead relies on the intake and ejection of a high-velocity working fluid through a solitary aperture. This process ensures that there is no overall mass flow. This study examined the effect of the volume cavity at varying distances from the nozzle to the heated surface, and at varying frequencies. In this study, three experiments involving heater characteristics, external and internal temperatures, and fluid air velocity for the manufactured synthetic jet were conducted by utilizing a 100-watt, 24-volt heater. The power input was set to achieve a consistent heater surface temperature at 343.15 K. Five different volumes were tested in the range of 300 Hz to 700 Hz driving frequency at a distance of 50 mm between the nozzle and the heated surface. Compared to other driving frequencies, it was observed that 500 Hz in Model 1 (431.75 K) produced the highest cooling effect by reducing the greatest temperature drop. It is assumed that the resonance frequency with the greatest amplitude is 500 Hz. The highest temperature decrease was obtained at a 50 mm distance. The maximum air velocity for each model was measured at 10 mm, while the lowest air velocity was obtained at a 70 mm distance. Model 1 of the synthetic jet produced the highest and lowest air velocity of 1.29 and 0.08 metres per second, respectively.

Keywords: *Electronic cooling, synthetic jet device, zero net mass flux, jet device*

1.0 INTRODUCTION

Every electronic device will fail as a result of high temperature or an overheating process. The device will burn or catch fire if heat is not dissipated efficiently[1] If the temperature continues to rise, even if it is not high enough to cause a fire or a device to catch fire, the high temperature may still cause a failure. Meanwhile, failures of microelectronic devices that are reliant on temperature are commonly classified as mechanical, corrosion, and electrical failures. [1]. The term "mechanical failure" encompasses instances of significant deformation, yielding, cracking, or fracturing in a material, as well as the detachment of a joint connecting two components. [1]. A material fails when subjected to a force that exceeds its yield stress in terms of force per unit area. In such cases, the joint connecting two components becomes incapable of withstanding the shear or tensile stress imposed, or fatigue failure occurs when a small force is repeatedly applied. Utilising appropriate heat transfer technology to remove internally generated heat as efficiently as possible in order to maintain component temperatures within safe operating limits is an absolute requirement for modern electronic devices.

 DOI: https://doi.org/10.11113/jm.v46.498

Thus, a variety of cooling technologies have been utilised to dissipate heat from electronic devices, including heat pipes, liquid cooling, vapour chambers, and synthetic jets. Heat pipes used to cool the electronic device can assist in transferring heat from its source to a location where it can be dissipated, thereby reducing the thermal resistance that spreads. A liquid-cooled system incorporates a liquid-cooled heat exchanger into the heat source to extract heat and lower air temperature. The widespread use of vapour chambers in electronic cooling allows for more uniform heat flux distribution and improved heat sink dissipation. The three primary components of a synthetic jet are the orifice, the chamber, and the oscillating driver. The common components of a synthetic jet are depicted in Figure 1. The oscillating driver plays a crucial role in the synthetic jet because it controls the jet's intensity and frequency [2].

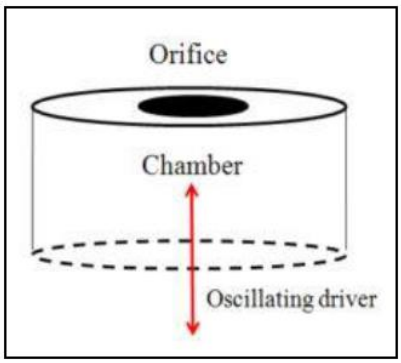

Figure 1: Schematic Diagram for Synthetic Jet [2]

According to [3], the membrane oscillation generates fluid movement into and out of the cavity through the orifice. Under specific operational conditions, in the absence of jet formation and diaphragm reversal, the discharged fluid is promptly recirculated into the cavity. However, when the amplitude and frequency of oscillation are optimal, separation of the ejected fluid occurs at the orifice's outer edges. The operation of a synthetic jet is based on the intake and ejection of high-velocity working fluid through a single orifice. Zero net mass flux results from the ingress and egress of high-velocity working fluid through a single aperture in synthetic jets [4]. Vortex interaction creates a zero-net-mass-flux jet with non-zero mean stream-wise momentum.

According to [3], a synthetic jet is a zero-net mass flux device capable of inducing non-zero momentum along the jet's direction. Figure 2 illustrates the ejection and suction operation of a synthetic jet device. Due to their ability to direct airflow along the heated surfaces in confined environments and to induce small-scale mixing, synthetic jets are better suited for cooling applications at the package and heat sink levels than other existing methods [1]. Synthetic jets have lower noise, power consumption, flexibility, reliability, miniaturisation, and fouling than conventional fans.

DOI: https://doi.org/10.11113/jm.v46.498

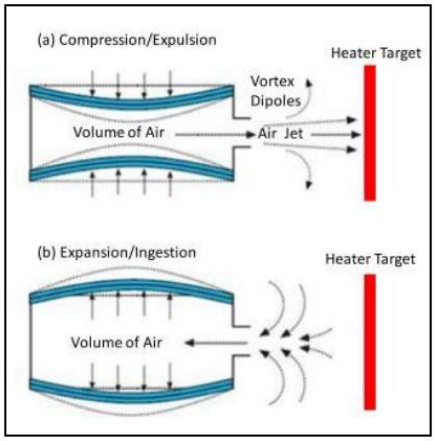

Figure 2: Synthetic Jet Ejection/Suction Phase [7]

The oscillating driver plays a crucial role in the synthetic jet because it controls the jet's frequency and strength [2] Common oscillating diaphragm types include motor-driven pistons, piezoelectric diaphragm, and acoustic excitation [4]. It suggests that in this regard, the type of device used to set the fluid in motion (loudspeaker, piezoelectric transducer) is more important than the arrangement of fins in the cavity.

Other recent studies suggest that the type of device used to move the fluid (loudspeaker, piezoelectric transducer) is more important than cavity fins. The impact of fins on the efficiency of Synthetic Jet Actuators (SJA) is relatively insignificant when compared to the greater significance of device types [5]. Recently, a study on the effects of thermal, flow, and acoustic characteristics in different geometry of loudspeaker-driven synthetic jets has found that the best cooling performance is found at the resonance frequency, however, the different numbers of orifices also affect the overall performance. [6]

Despite the fact that numerous studies have been conducted, a study focusing on the effect of air volume at different distances on thermal cooling pumping jet devices has been overlooked. Therefore, this study will focus on investigating the effects of volume cavities at varying frequencies in cooling applications. Next, an experiment would be conducted to determine the temperature and velocity for each swept volume using a synthetic jet with varying swept volumes. The determination of the coefficient of heat transfer will conclude the process.

2.0 METHODOLOGY

2.1 Experiment configurations

The study included heater characteristics, nozzle-heated surface temperature distance, and fluid velocity frequency studies. The heater characteristic experiment is employed to determine the relationship between the heater's power and temperature using a 24V voltage and 100W of power. Subsequently, a synthetic jet experiment was carried out to ascertain the effect of temperature at different distances from the nozzle to the heated surface temperature. In addition, the synthetic jet was tested at various frequencies ranging from 300 Hz to 700 Hz at a distance of 50 mm from the nozzle to the heated surface temperature. Throughout the course of this study, five different cavity depth values will be incorporated into the design of synthetic jet models. Table 1 displays the configuration design of the synthetic jet, while Table 2 lists the equipment and the configurations of the experiment.

DOI: https://doi.org/10.11113/jm.v46.498

Table 1: Synthetic Jet Design's Configuration

Model	Depth of Cavity (H)	Diameter of Cavity (Dc)	Diameter of Orifice (Do)	Volume of Model (V)
MODEL 1	1mm	40 mm	2mm	1.26 X 10-6 m
MODEL 2	2mm	40mm	2mm	2.51 X 10-6 m
MODEL 3	3mm	40mm	2mm	3.77 X 10-6 m
MODEL 4	4mm	40mm	2mm	5.03 X 10-6 m
MODEL 5	5mm	40mm	2mm	6.28 X 10-6 m

Table 2: List of equipment and its configurations

Equipment	Functions and Settings
DC Power Supply	Voltage: 6.8 V Current: 2.1 A
Portable Data Acquisition Module	Measure the temperature of the ambient and the heater.
Thermocouple Cable (Type K)	**Function:** Use to measure the heater's temperature and the ambient temperature **Setting:** The ambient temperature is measured at channel 0 of the Data Acquisition Module while the heater temperature is measured at channel 2.
Heater 24 V :100W	**Function:** To generate heat capable of consuming 24 volts and 100 watts of energy when a current of 4 amps flows through it. **Setting:** Adjust the voltage and current values until the heater temperature reaches 343.15 Kelvin.
Cable Clip	**Function:** To connect the circuit between DC Power Supply to the heater
Function Generator:	**Function:** Used to generate the frequency signal to oscillate the diaphragm of synthetic jet. **Setting:** After the heated surface's temperature reaches 343.15 K, activate the function generator. 900 seconds must pass until the temperature remains constant.
Oscilloscope	**Function:** To observe the constantly varying signal voltages usually as a two- dimensional plot.
Retort Stand and Clamp	**Function:** Used to adjust the distance between the nozzle jet to the heated surface temperature.
Synthetic Jet Actuator	**Function**: Consists of cavity volume, piezoelectric diaphragm and orifice that are used for ejection and suction heat from the heater **Setting:** Connect the piezoelectric diaphragm to the function generator for the diaphragm to oscillate when the heater temperature reaches 343.15 K.
Hot Wire Anemometer	**Function:** Used to collect data for air velocity of synthetic jet actuator. **Setting:** Connect the hot wire to the DAQ and ensure that the initial velocity value is 0 m/s. Wait 900 seconds before gathering air velocity data.

The synthetic jet actuator was fabricated by using 3D Printing as shown in Figure 3. The material used for the synthetic jet is plastic. Diameter of Orifice (Do) and Diameter of Cavity (Dc) are shown in Figure 3a) and 3c), fixedly set at 2mm and 40mm respectively, in all 5 models. The value of Depth Cavity, H as shown in Figure 3b) is varied from 1mm to 5mm as depicted in Table 1.

DOI: https://doi.org/10.11113/jm.v46.498

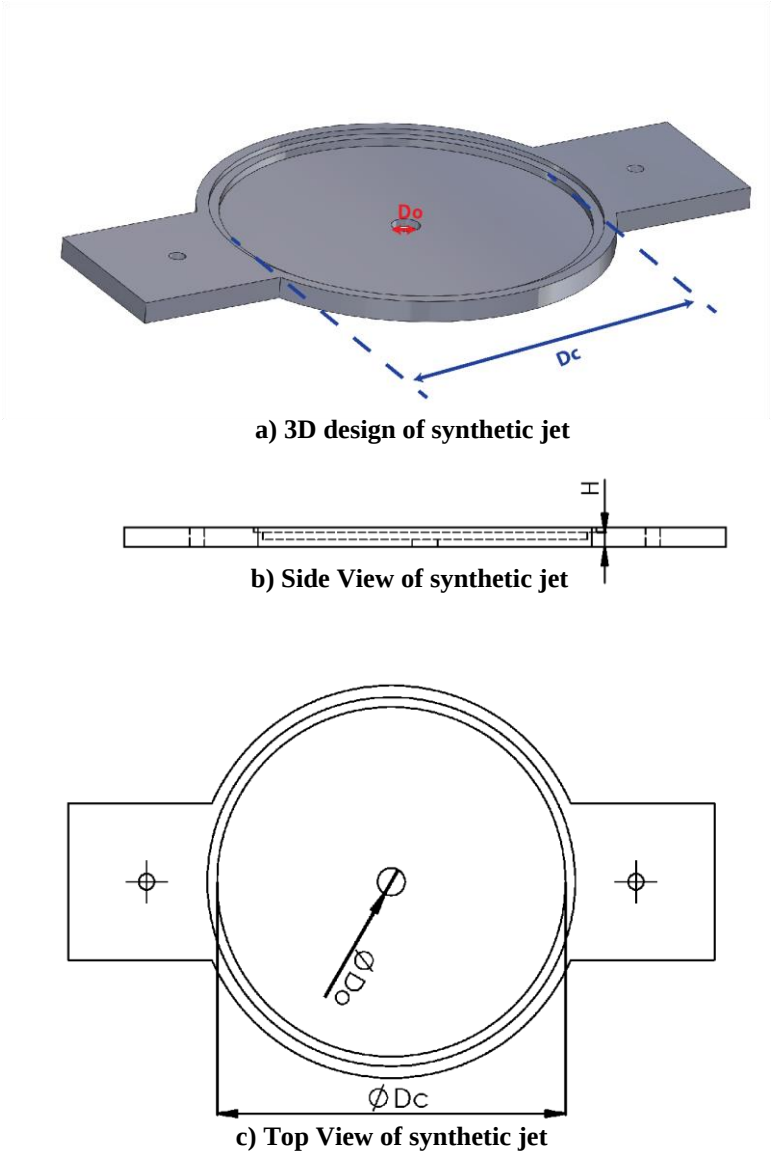

a) 3D design of synthetic jet

b) Side View of synthetic jet

c) Top View of synthetic jet

Figure 3: a) Design of synthetic jet in 3D; b) Schematic Design from the side and; c)top view

2.2 Heater Characteristics Experiment

This experiment was conducted to determine the relationship between 24V: 100W heater power supply and temperature. The heater received its voltage (V) and current (Amp) from the DC power supply. The Data Acquisition module (DAQ) and thermocouple wire were utilised to measure and record the heater's temperature to obtain 343.15 K, as this temperature is the common maximum temperature in electronic devices. As shown in Figure 4, the thermocouple was placed below the position of the heater.

DOI: https://doi.org/10.11113/jm.v46.498

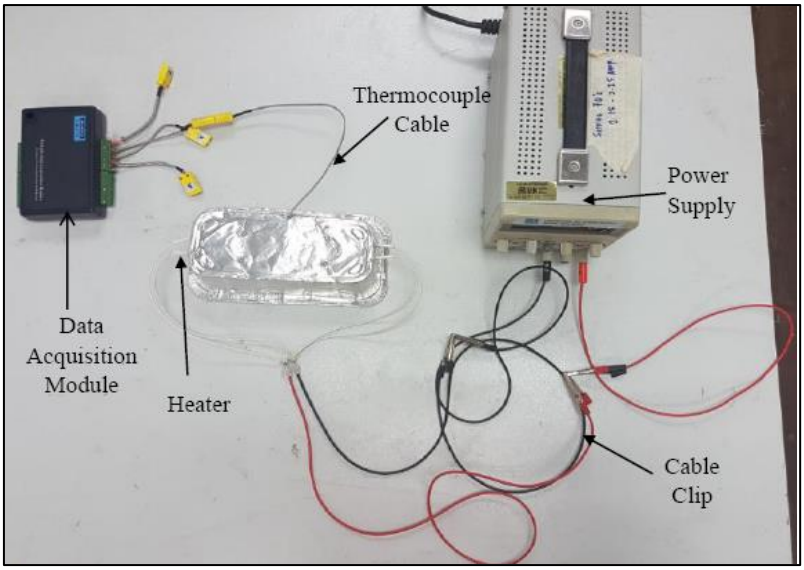

Figure 4: Setup of Heater Characteristics Experiment

2.3 Heat Dissipation Experiment

This experiment was conducted to determine, based on the cavity volume, the heat dissipation of a synthetic jet. The arrangement is depicted in Figure 5. For the experiment, the cavity synthetic jet depth ranged from 1 millimetre to 5 millimetres. The best distance for the synthetic jet actuator was also determined by analysing a variety of distances between the nozzle jet and the heated surface temperature. In accordance with the experimental design, a regulated voltage (V) and current (Amp) resulted in a surface temperature of 343.15 K. Then, after a period of time in which the heater reached a temperature of 343.15 K, the experiment of a synthetic jet with an applied frequency of 500 Hz caused the oscillation of the synthetic jet's diaphragm. The experiment was repeated with the distance between the synthetic jet nozzle and the heated surface varying from 30 to 70 millimetres.

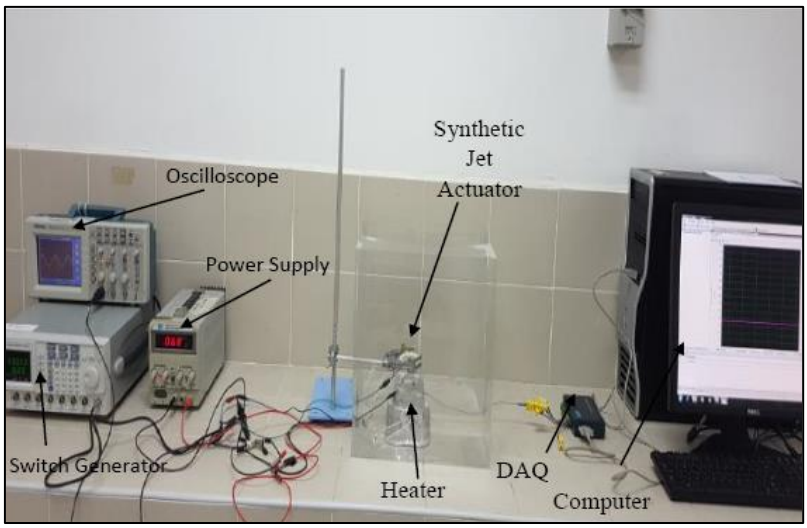

Figure 5: Experiment setup of Heat Dissipation for Synthetic Jet

DOI: https://doi.org/10.11113/jm.v46.498

2.4 Fluid Velocity Experiment of Synthetic Jet

This experiment measures the fluid velocity of a synthetic jet at varying distances from the nozzle jet to the heated surface. In the experiment, various cavity depths in synthetic jets, as listed in Table 3.0, were examined. Furthermore, at a frequency of 500 Hz, different distances between the nozzle jet and the heated surface were determined. Equipment such as a hot wire anemometer was used to determine the velocity values when 500 Hz was applied to the synthetic jet. In addition, the software of the desktop-connected hot wire anemometer was used to record the values of the synthetic jet velocity. Each test required 15 minutes for every 500 Hz frequency applied. A full experiment setup is shown in Figure 6.

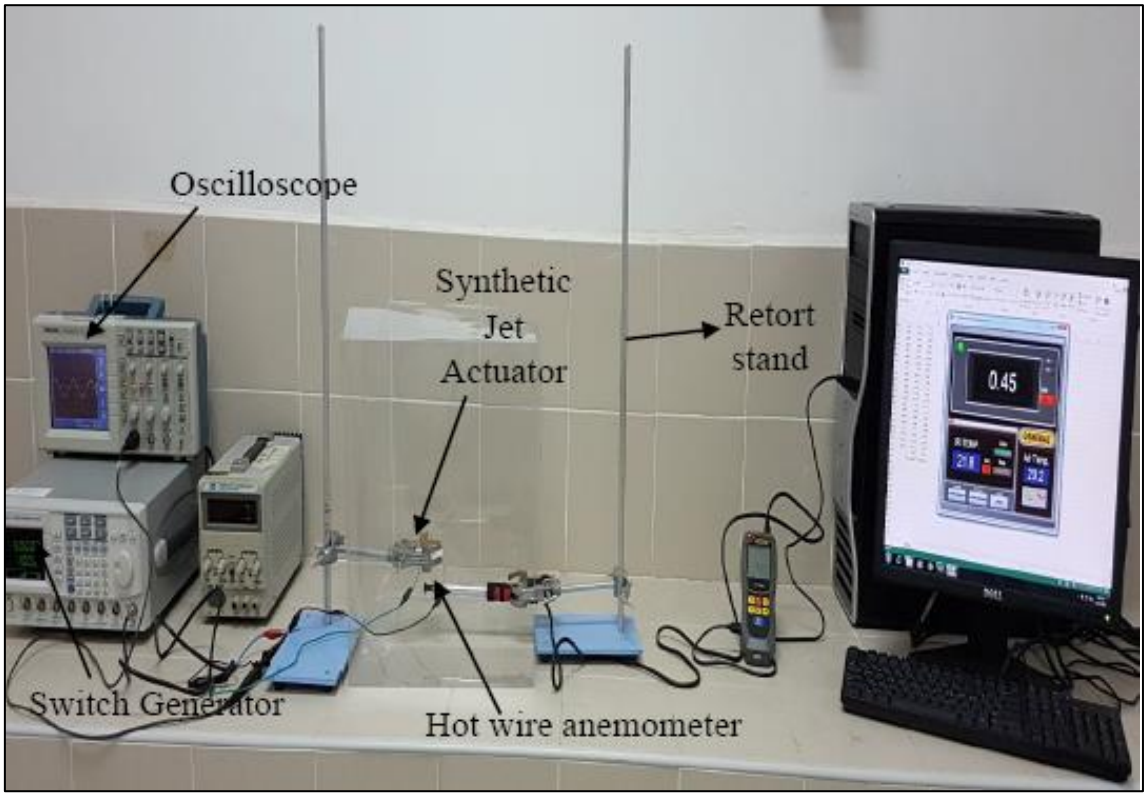

Figure 6: Experiment setup of Fluid Velocity Experiment

3.0 RESULTS AND DISCUSSION

3.1 Heater Characteristics

Figure 7 and Table 3 depict the relationship between temperature (T) in Kelvin (K) and power (P) in Watts (W). The graph clearly demonstrates a proportional increase in temperature with increasing power. The heater's temperature at zero watts was 295.54 Kelvin, the same as the ambient temperature. The surface temperature of a 24V, 100W heater reached 343,15K when the voltage was 6.80 V and the current was 2.10 Amps. The heater reaches a maximum temperature of 353.81 Kelvin.

DOI: https://doi.org/10.11113/jm.v46.498

Table 3: Data for Heater 24V:100W

Voltage, (v)	Current (A)	Power (W)	Temperature (K)
0	0.00	0.00	295.54
1	0.33	0.33	299.59
2	0.57	1.14	305.26
3	0.70	2.10	313.88
4	1.24	4.96	319.71
5	1.46	7.30	325.75
6	2.03	12.18	336.93
7	2.32	16.24	350.11
8	2.65	21.20	353.81

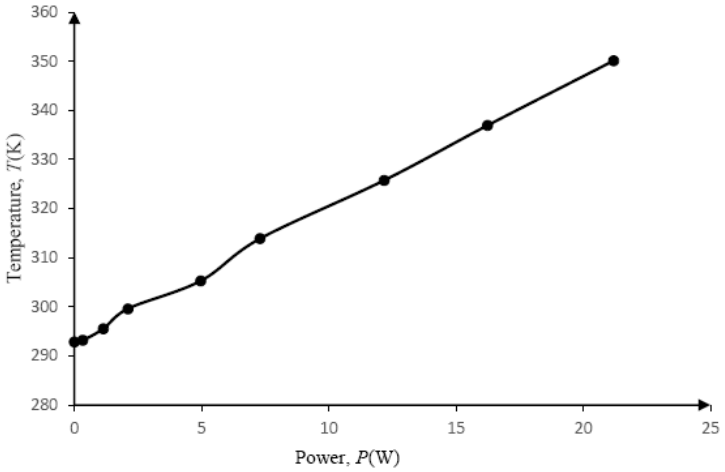

Figure 7 : Temperature, *T*(K) vs Power,*P* (W)

3.2 Impact of Diverse Distances Between the Heated Surface and the Nozzle Jet

The distance, z, from the nozzle to the heated surface temperature of Model 5 (as shown in Table 1) was set. As depicted in Figure 8, all distances were able to reduce the initial surface temperature of 343.15 K and maintain the temperature values after 400 seconds. At 50 mm, the maximum temperature decreases from the heated surface temperature to 334.96 K, while at 70 mm, the minimum temperature decreases to 342.51 K.

DOI: https://doi.org/10.11113/jm.v46.498

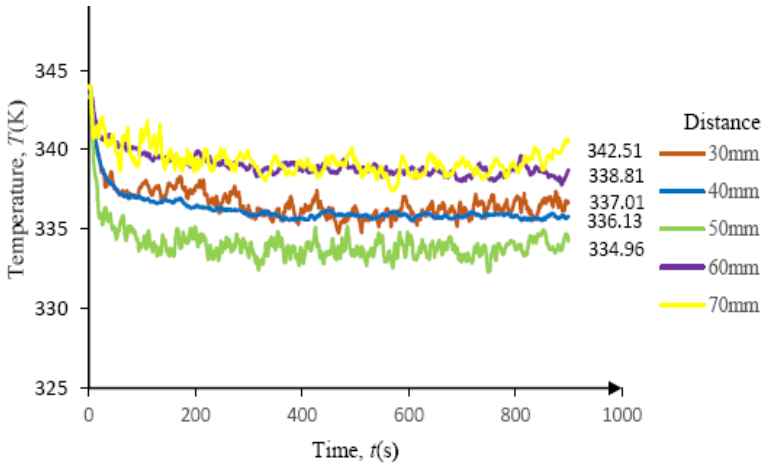

Figure 8: Model 5 at Various Distance of Temperature (K) vs Time (s)

Figure 9 depicts the heat transfer coefficient, h (W/m2.K), for all models at various distances. All models exhibit the same trend or result for the heat transfer coefficient, h, at various distances, namely that as the volume increases, the coefficient decreases. The maximum value at a distance of 50 mm for all models of heat transfer coefficient, h. At each distance, Model 1 has the largest value of the heat transfer coefficient, denoted as h., while Model 5 exhibits the minimum value over all distances. As a result, the heat transfer coefficient, denoted as h, peaked at 431.75 (W/m2.K) at a distance of 50 mm and plummeted to 305.65 (W/m2.K) at 70 mm.

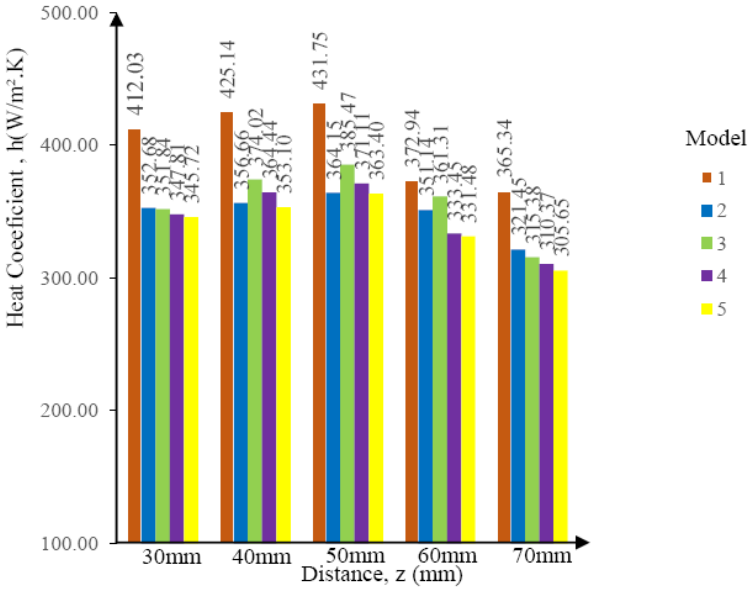

Figure 9: Heat Transfer Coefficient, *h* (W/m².K) vs. Distance, *z* (mm)

3.32 Effect of Various Frequency to the Synthetic Jet Performance

Each form of synthetic jet is illustrated in Figure 10 at a distance of 50 mm for each frequency. In comparison to other frequencies, 500 Hz was able to reduce maximum heat because this frequency was fundamental to the resonance frequency, the maximum amplitude of the diaphragm fluctuates. According to [7], at the resonance frequency, heat transfer reaches its maximum values.

DOI: https://doi.org/10.11113/jm.v46.498

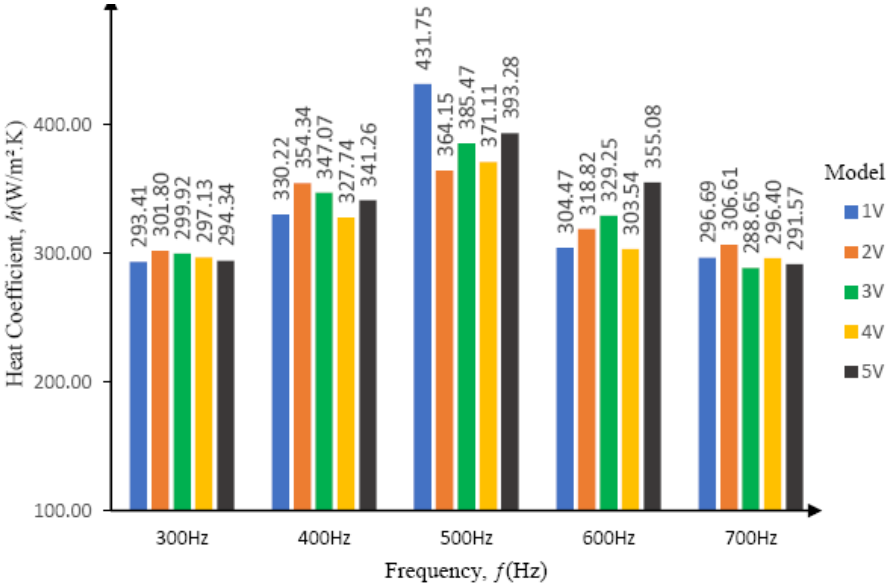

Figure 10: All models at a distance of 50mm in different frequencies

3.33 Fluid Velocity at Various Frequencies

The velocity, v (m/s), at different distances for all synthetic jet models is illustrated in Figure 11. When the distance between the nozzle and the anemometer wire was small, the synthetic jet achieved its maximum velocity. The minimum air velocity recorded for each kind of synthetic jet was 70 mm, whilst the maximum air velocity was 10 mm. The maximum air velocity recorded for Model 1 of the synthetic jet was 1.29 m/s, while the minimum air velocity was 0.08 m/s.

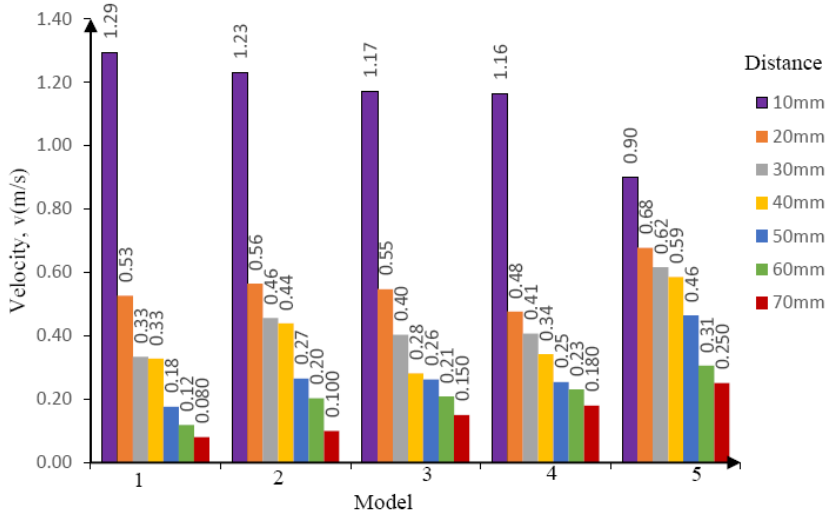

Figure 11: Velocity (m/s) values in all models

DOI: https://doi.org/10.11113/jm.v46.498

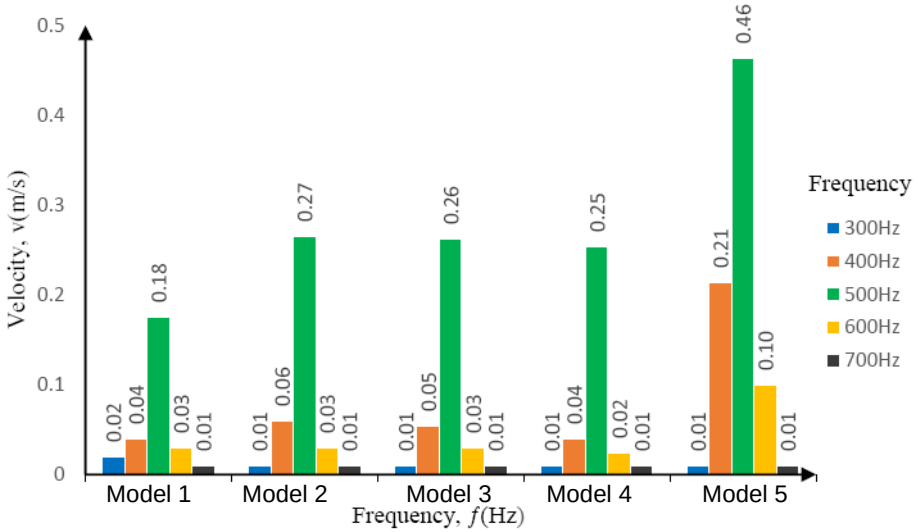

Figure 12: Velocity (m/s) for various Frequency (Hz) at a Distance of 50mm

The frequency of 500 Hz has the highest velocity for each model of synthetic jet, as shown in Figure 12. 700 Hz is the lowest velocity value. According to [6], a vortex flow tends to disperse and form secondary flow structures at higher driven frequencies, resulting in a decrease in velocity. Consequentially, at 500 Hz, the value of model 5 indicates that the maximum air velocity is 0.46 m/s, while the minimum air velocity at 700 Hz is 0.01 m/s, which is consistent with the findings of the previous researcher.

4.0 CONCLUSION

Frequencies ranging from 300 Hz to 700 Hz are utilised to calculate the heat transfer coefficient and fluid velocity. In comparison to other frequencies, the heat transfer coefficients and fluid air velocity are greatest at 500 Hz. The maximum amplitude of an oscillating diaphragm occurred when its frequency reached resonance. The synthetic jet cavity with the smallest volume produced the highest heat transfer coefficient compared to the cavity with the largest volume.

It is observed that the effect of frequency on synthetic jet actuators produced a significant cooling effect than the parameters of distance and volume. However, the distance between the synthetic jet and the heater surface also influences the value of heat transfer coefficients as it is found that the maximum heat transfer coefficient is obtained at a distance of 50 mm from the nozzle jet to the heated surface.

Model 1, which has the lowest air volume produced the highest heat transfer coefficient, h, at every distance compared to other models. Meanwhile, Model 5 which has the highest air volume produced the lowest heat transfer coefficient, h compared to other models. In conclusion, the smaller cavity volume produced better cooling performance compared to the larger cavity volume in the synthetic jet devices as observed in this experiment.

ACKNOWLEDGMENT

The author wishes to express gratitude to UiTM and the Research Acculturation Grant Scheme (RAGS) from the Malaysia Higher Education Department (Grant No. 600-RMI/RAGS 5/3 (217/2014)) for funding this study.

DOI: https://doi.org/10.11113/jm.v46.498

REFERENCES

1. Y. Shabany, *Heat Transfer*. CRC Press, 2009. doi: 10.1201/9781439814680.
2. Hoda Eiliat, "Experimental Study of Synthetic Jets," *Electronic Theses and Dissertations*, 2009.
3. C. Y. Y. Lee, M. L. Woyciekoski, and J. B. Copetti, "Experimental study of synthetic jets with rectangular orifice for electronic cooling," *Exp Therm Fluid Sci*, vol. 78, pp. 242–248, Nov. 2016, doi: 10.1016/j.expthermflusci.2016.06.007.
4. N. Dahalan, S. Mansor, M. Haniff Shaharudin, and A. Ali, "Evaluation of synthetic jet actuators design performance," *Aircraft Engineering and Aerospace Technology*, vol. 84, no. 6, pp. 390–397, Oct. 2012, doi: 10.1108/00022661211272909.
5. E. Smyk, P. Gil, R. Gałek, and Ł. Przeszłowski, "Acoustic and Flow Aspects of Novel Synthetic Jet Actuator," *Actuators*, vol. 9, no. 4, p. 100, Oct. 2020, doi: 10.3390/act9040100.
6. P. Gil, E. Smyk, R. Gałek, and Ł. Przeszłowski, "Thermal, flow and acoustic characteristics of the heat sink integrated inside the synthetic jet actuator cavity," *International Journal of Thermal Sciences*, vol. 170, p. 107171, Dec. 2021, doi: 10.1016/J.IJTHERMALSCI.2021.107171.
7. M. Girfoglio, C. S. Greco, M. Chiatto, and L. de Luca, "Modelling of efficiency of synthetic jet actuators," *Sens Actuators A Phys*, vol. 233, pp. 512–521, Sep. 2015, doi: 10.1016/j.sna.2015.07.030.
8. O. Ghaffari, S. A. Solovitz, and M. Arik, "An investigation into flow and heat transfer for a slot impinging synthetic jet," *Int J Heat Mass Transf*, vol. 100, pp. 634–645, Sep. 2016, doi: 10.1016/j.ijheatmasstransfer.2016.04.115.
9. M. N. Dahalan, S. Mansor, and A. Ali, "Cavity Effect of Synthetic Jet Actuators Based on Piezoelectric Diaphragm," *Applied Mechanics and Materials*, vol. 225, pp. 85–90, Nov. 2012, doi: 10.4028/www.scientific.net/AMM.225.85.
10. U. S. Bhapkar, A. Srivastava, and A. Agrawal, "Acoustic and heat transfer characteristics of an impinging elliptical synthetic jet generated by acoustic actuator," *Int J Heat Mass Transf*, vol. 79, pp. 12–23, Dec. 2014, doi: 10.1016/j.ijheatmasstransfer.2014.07.083.
11. X. He, J. A. Lustbader, M. Arik, and R. Sharma, "Heat transfer characteristics of impinging steady and synthetic jets over vertical flat surface," *Int J Heat Mass Transf*, vol. 80, pp. 825–834, Jan. 2015, doi: 10.1016/j.ijheatmasstransfer.2014.08.006.
12. Y.-H. Liu, S.-Y. Tsai, and C.-C. Wang, "Effect of driven frequency on flow and heat transfer of an impinging synthetic air jet," *Appl Therm Eng*, vol. 75, pp. 289–297, Jan. 2015, doi: 10.1016/j.applthermaleng.2014.09.086.
13. M. Ja'fari, F. J. Shojae, and A. J. Jaworski, "Synthetic jet actuators: Overview and applications," *International Journal of Thermofluids*, vol. 20, p. 100438, Nov. 2023, doi: 10.1016/j.ijft.2023.100438.
14. Y. Kang *et al.*, "Numerical study of a liquid cooling device based on dual synthetic jets actuator," *Appl Therm Eng*, vol. 219, p. 119691, Jan. 2023, doi: 10.1016/j.applthermaleng.2022.119691.
15. M. Chaudhari, B. Puranik, and A. Agrawal, "Effect of orifice shape in synthetic jet based impingement cooling," *Exp Therm Fluid Sci*, vol. 34, no. 2, pp. 246–256, Feb. 2010, doi: 10.1016/j.expthermflusci.2009.11.001.
16. U. S. Bhapkar, A. Srivastava, and A. Agrawal, "Proper cavity shape can mitigate confinement effect in synthetic jet impingement cooling," *Exp Therm Fluid Sci*, vol. 68, pp. 392–401, Nov. 2015, doi: 10.1016/j.expthermflusci.2015.05.006.
17. K. Kim, P. Pokharel, and T. Yeom, "Enhancing forced-convection heat transfer of a channel surface with synthetic jet impingements," *Int J Heat Mass Transf*, vol. 190, p. 122770, Jul. 2022, doi: 10.1016/J.IJHEATMASSTRANSFER.2022.122770.
18. P. Gil, "Flow and heat transfer characteristics of single and multiple synthetic jets impingement cooling," *Int J Heat Mass Transf*, vol. 201, p. 123590, Feb. 2023, doi: 10.1016/J.IJHEATMASSTRANSFER.2022.123590.
19. S. Yuura, Y. Watanabe, K. Furutani, and T. Handa, "Ultrasonic-driven synthetic-jet actuator: High-efficiency actuator creating high-speed and high-frequency pulsed jet," *Sens Actuators A Phys*, vol. 353, p. 114231, Apr. 2023, doi: 10.1016/J.SNA.2023.114231.
20. V. Arumuru, K. Rajput, R. Nandan, P. Rath, and M. Das, "A novel synthetic jet based heat sink with PCM filled cylindrical fins for efficient electronic cooling," *J Energy Storage*, vol. 58, p. 106376, Feb. 2023, doi: 10.1016/J.EST.2022.106376.
21. W. He *et al.*, "Numerical study on the atomization mechanism and energy characteristics of synthetic jet/dual synthetic jets," *Appl Energy*, vol. 346, p. 121376, Sep. 2023, doi: 10.1016/J.APENERGY.2023.121376.
22. M. Ja'fari, F. J. Shojae, and A. J. Jaworski, "Synthetic jet actuators: Overview and applications," *International Journal of Thermofluids*, vol. 20, Nov. 2023, doi: 10.1016/j.ijft.2023.100438.
23. J. W. Tan, J. Z. Zhang, Y. W. Lyu, and J. Yang Zhang, "Experimental study on convective heat transfer of hybrid impingement configuration by square-array continuous jets and a center-positioned synthetic jet," *Int J Heat Mass Transf*, vol. 215, p. 124414, Nov. 2023, doi: 10.1016/J.IJHEATMASSTRANSFER.2023.124414.
24. B. Gungordu, M. Jabbal, and A. A. Popov, "Structural–fluidic–acoustic computational modeling and experimental validation of piezoelectric synthetic jet actuators," *Int J Heat Fluid Flow*, vol. 104, p. 109215, Dec. 2023, doi: 10.1016/J.IJHEATFLUIDFLOW.2023.109215.
25. G. E. Lau, J. Mohammadpour, and A. Lee, "Cooling performance of an impinging synthetic jet in a microchannel with nanofluids: An Eulerian approach," *Appl Therm Eng*, vol. 188, p. 116624, Apr. 2021, doi: 10.1016/J.APPLTHERMALENG.2021.116624.
26. P. Gil, J. Wilk, R. Smusz, and R. Gałek, "Centerline heat transfer coefficient distributions of synthetic jets impingement cooling," *Int J Heat Mass Transf*, vol. 160, p. 120147, Oct. 2020,

 DOI: https://doi.org/10.11113/jm.v46.498

doi: 10.1016/J.IJHEATMASSTRANSFER.2020.120147.
27. P. Gil, "Experimental investigation on heat transfer enhancement of air-cooled heat sink using multiple synthetic jets," *International Journal of Thermal Sciences*, vol. 166, p. 106949, Aug. 2021, doi: 10.1016/J.IJTHERMALSCI.2021.106949.
28. Z. Luo, W. He, X. Deng, M. Zheng, T. Gao, and S. Li, "A compacted non-pump self-circulation spray cooling system based on dual synthetic jet referring to the principle of two-phase loop thermosyphon," *Energy*, vol. 263, p. 125757, Jan. 2023, doi: 10.1016/J.ENERGY.2022.125757.

 DOI: https://doi.org/10.11113/jm.v46.498